nature immunology

S6K-STING interaction regulates cytosolic DNA–mediated activation of the transcription factor IRF3

Fuan Wang[1,2], Tommy Alain[3], Kristy J Szretter[4], Kyle Stephenson[1,2], Jonathan G Pol[1,2], Matthew J Atherton[1,2], Huy-Dung Hoang[3], Bruno D Fonseca[3], Chadi Zakaria[5], Lan Chen[1,2], Zainab Rangwala[1,2], Adam Hesch[1,2], Eva Sin Yan Chan[1,2], Carly Tuinman[1,2], Mehul S Suthar[6], Zhaozhao Jiang[7], Ali A Ashkar[1,2], George Thomas[8–10], Sara C Kozma[8,9], Michael Gale Jr[11], Katherine A Fitzgerald[7], Michael S Diamond[4], Karen Mossman[1,2], Nahum Sonenberg[5], Yonghong Wan[1,2,12] & Brian D Lichty[1,2,12]

Cytosolic DNA–mediated activation of the transcription factor IRF3 is a key event in host antiviral responses. Here we found that infection with DNA viruses induced interaction of the metabolic checkpoint kinase mTOR downstream effector and kinase S6K1 and the signaling adaptor STING in a manner dependent on the DNA sensor cGAS. We further demonstrated that the kinase domain, but not the kinase function, of S6K1 was required for the S6K1-STING interaction and that the TBK1 critically promoted this process. The formation of a tripartite S6K1-STING-TBK1 complex was necessary for the activation of IRF3, and disruption of this signaling axis impaired the early-phase expression of IRF3 target genes and the induction of T cell responses and mucosal antiviral immunity. Thus, our results have uncovered a fundamental regulatory mechanism for the activation of IRF3 in the cytosolic DNA pathway.

In eukaryotic cells, double-stranded DNA is normally sequestered in the nucleus or the mitochondria and is thereby prevented from direct contact with the cytosol. Thus, cytosolic exposure of DNA resulting from microbial infection or damaged host cells turns on an evolutionarily conserved 'danger' signal to alarm the host immune system[1,2]. In particular, infection with various DNA virus families results in the introduction of DNA into the cytosol. For example, adenovirus (Ad), a nonenveloped, double-stranded DNA virus used extensively as a vector for both gene therapy and DNA vaccines[3], exposes its genomic DNA to the cytosol during the infection process and has been used as a prototypical DNA virus for the study of DNA-recognition pathways of the host innate immune system[4,5].

Cytosolic DNA is a key pathogen-associated molecular pattern that is sensed mainly through the cytosolic cyclic GMP-AMP (cGAMP) synthase cGAS[6,7], which triggers innate antiviral and autoimmune responses[1,2]. Upon binding to cytosolic DNA, cGAS catalyzes the production of a secondary messenger, the noncanonical 2′,3′ cGAMP (c[G(2′,5′)pA(3′,5′)p]), which is distinct from the canonical bacterial 3′,3′ cGAMP (c[G(3′,5′)pA(3′,5′)p])[6–9]. The cGAS product binds to and activates the downstream signaling adaptor STING[10,11] (also known as MPYS, MITA, ERIS and TMEM173)[12–15]. Activated STING in turn recruits and activates the transcription factor NF-κB inhibitor IκB kinase IKK and the kinase TBK1, which leads to activation of NF-κB and the transcription factor IRF3, respectively[6,7,9]. Despite such advances in the understanding of DNA-sensing mechanisms, the interactions between distinct regulatory molecules involved in the cytosolic DNA–signaling machinery remain to be further defined.

The two homologous isoforms of the ribosomal protein S6 kinase (S6K), S6K1 and S6K2, are effector serine-threonine kinases downstream of mTOR, a central member in the family of kinase PI(3)K–related kinases that functions as a key signaling integrator of a variety of cues, such as nutrients, stress, cell growth and apoptosis, and transcriptional as well as translational coordination[16]. Of importance, published studies have shown that the mTOR-S6K signaling axis modulates Toll-like receptor pathways in a manner sensitive to the mTOR inhibitor rapamycin[17–19]. However, it is currently unknown whether mTOR-S6K is integrated into the cytosolic DNA–mediated STING signalosome.

Here, using Ad as a model DNA virus, we found that S6Ks, especially S6K1, were required for Ad-induced activation of IRF3 independently

[1]McMaster Immunology Research Centre, Department of Pathology and Molecular Medicine, McMaster University, Hamilton, Canada. [2]MG DeGroote Institute for Infectious Disease Research, McMaster University, Hamilton, Canada. [3]Children's Hospital of Eastern Ontario Research Institute and Department of Biochemistry, Microbiology, and Immunology, University of Ottawa, Ottawa, Canada. [4]Department of Medicine, Molecular Microbiology, Pathology & Immunology, Washington University School of Medicine, St Louis, Missouri, USA. [5]Department of Biochemistry and Goodman Cancer Research Centre, McGill University, Montreal, Canada. [6]Department of Pediatrics, Emory Vaccine Center, Emory University, Atlanta, Georgia, USA. [7]Division of Infectious Diseases and Immunology, Department of Medicine, University of Massachusetts Medical School, Worcester, Massachusetts, USA. [8]Department of Internal Medicine, Division of Hematology/Oncology, University of Cincinnati Medical School, Cincinnati, Ohio, USA. [9]Laboratory of Metabolism and Cancer, Catalan Institute of Oncology, ICO, Bellvitge Biomedical Research Institute, IDIBELL, Barcelona, Spain. [10]Departament Ciències Fisiològiques II, Facultat de Medicina, Universitat de Barcelona, Barcelona, Spain. [11]Department of Immunology, University of Washington School of Medicine, Seattle, Washington, USA. [12]These authors contributed equally to this work. Correspondence should be addressed to B.D.L. (lichtyb@mcmaster.ca).

Received 31 December 2015; accepted 8 March 2016; published online 4 April 2016; doi:10.1038/ni.3433

of the kinase activity of S6K. We demonstrated that S6K1 interacted physically with activated STING in a cGAS-cGAMP–dependent manner and formed a tripartite S6K1-STING-TBK1 signaling complex. This S6K-dependent IRF3 signaling was important for the induction of early innate immune responses, as well as robust T cell immunity and mucosal antiviral defense. Thus, our report reveals a previously unrecognized regulatory function of S6Ks in the context of cytosolic DNA–elicited immunological signaling.

RESULTS

Requirement for S6K1 and S6K2 in Ad-induced IRF3 activation

Ad induces the phosphorylation of IRF3 in a variety of immune cells[4,5]. To characterize the profile of Ad-induced IRF3 phosphorylation in mouse bone marrow–derived myeloid dendritic cells (BMDCs), we transduced wild-type BMDCs with recombinant human Ad serotype 5 vector with deletion of E1 and E3, which are involved in mediating Ad replication and host immunomodulation, respectively. Immunoblot analysis showed that Ad elicited sustained phosphorylation of IRF3 at Ser396 over a time course of 48 h in BMDCs (**Supplementary Fig. 1a**) and that phosphorylated IRF3 was distributed in both nuclear fractions and cytoplasmic fractions (**Supplementary Fig. 1b**), which suggested that Ad-induced phosphorylation of IRF3 was a continual process in BMDCs.

IRF3 signaling is pivotal in host immune responses[20,21]. Because mTOR-S6K and mTOR–4E-BP signaling modules, widely known as regulators of cell growth and metabolism, have been shown to shape host innate immunity[17–19,22], we sought to determine whether S6K1 and S6K2 or members of the 4E-BP family of translational repressors were involved in regulating cytosolic DNA–induced phosphorylation of IRF3 by transducing Ad into BMDCs deficient in S6K1 (*Rps6kb1*$^{-/-}$; called '*S6k1*$^{-/-}$' here) or S6K2 (*Rps6kb2*$^{-/-}$; called '*S6k2*$^{-/-}$' here) or both (*S6k1*$^{-/-}$*S6k2*$^{-/-}$), or deficient in 4E-BP1 and 4E-BP2 (*Eif4ebp1*$^{-/-}$ *Eif4ebp2*$^{-/-}$) or 4E-BP1, 4E-BP2 and 4E-BP3 (*Eif4ebp1*$^{-/-}$*Eif4ebp2*$^{-/-}$*Eif4ebp3*$^{-/-}$). There was much less phosphorylation of IRF3 in *S6k1*$^{-/-}$ BMDCs (**Fig. 1b**) than in wild-type BMDCs (**Fig. 1a**), whereas the effect of the deletion of S6K2 was less severe (**Fig. 1c**). The phosphorylation of IRF3 was profoundly impaired in *S6k1*$^{-/-}$*S6k2*$^{-/-}$ BMDCs (**Fig. 1d**), while no such effect was observed in *Eif4ebp1*$^{-/-}$*Eif4ebp2*$^{-/-}$ or *Eif4ebp1*$^{-/-}$*Eif4ebp2*$^{-/-}$*Eif4ebp3*$^{-/-}$ BMDCs (**Supplementary Fig. 1c**). Notably, expression of IRF3 protein was not affected by ablation of S6K1 or S6K2 or both (**Fig. 1b–d**), which indicated that the regulation of Ad-induced activation of IRF3 by S6K was not due to downregulation of IRF3 expression. Furthermore, immunoblot analysis showed that Ad promoted translocation of IRF3 to the nucleus in wild-type BMDCs but not in *S6k1*$^{-/-}$*S6k2*$^{-/-}$ BMDCs (**Fig. 1e**). Immunofluorescence microscopy confirmed that the Ad-induced translocation of IRF3 to the nucleus was much lower in *S6k1*$^{-/-}$*S6k2*$^{-/-}$ BMDCs than in wild-type BMDCs (**Fig. 1f**). Together these results indicated that S6Ks, particularly S6K1, were essential for Ad-triggered activation of IRF3. Additionally, we observed that the phosphorylation of IRF3 induced by herpes simplex virus type 1 (HSV-1) was similarly lower in *S6k1*$^{-/-}$*S6k2*$^{-/-}$ BMDCs than in wild-type BMDCs (**Supplementary Fig. 2a**).

In parallel experiments, we stimulated wild-type and *S6k1*$^{-/-}$*S6k2*$^{-/-}$ BMDCs with lipopolysaccharide, which is a ligand for Toll-like receptor 4, or with vesicular stomatitis virus (VSV), which is known to activate the RNA helicase RIG-I[23]. We observed no difference between wild-type and *S6k1*$^{-/-}$*S6k2*$^{-/-}$ BMDCs in their phosphorylation of IRF3 after such treatment (**Supplementary Fig. 2b,c**), which suggested that S6K was required specifically for viral DNA–induced activation of IRF3 in the cytosolic DNA pathway. To extend these findings, we transfected purified Ad DNA, synthetic interferon-stimulatory DNA (ISD) or non-canonical cGAMP, the mammalian cGAS cyclic dinucleotide[8,24], into BMDCs. Transfection of Ad DNA (**Supplementary Fig. 3a**), ISD (**Supplementary Fig. 3b**) or cGAMP (**Supplementary Fig. 3c**) triggered robust phosphorylation of IRF3 in wild-type BMDCs but not in *S6k1*$^{-/-}$*S6k2*$^{-/-}$ BMDCs. Thus, S6K1 and S6K2 were essential for the cytosolic DNA–induced phosphorylation of IRF3.

Next we investigated the S6K-dependent induction of interferon-stimulated genes following transfection of ISD into BMDCs. Stimulation with ISD triggered robust induction of IFIT1, IFIT3 and ISG15 protein, all encoded by genes that are targets of IRF3, in wild-type BMDCs (**Supplementary Fig. 3d**). In contrast, 8-hour induction of these proteins was substantially impaired in both *S6k1*$^{-/-}$*S6k2*$^{-/-}$ BMDCs (**Supplementary Fig. 3e**) and IRF3-deficient

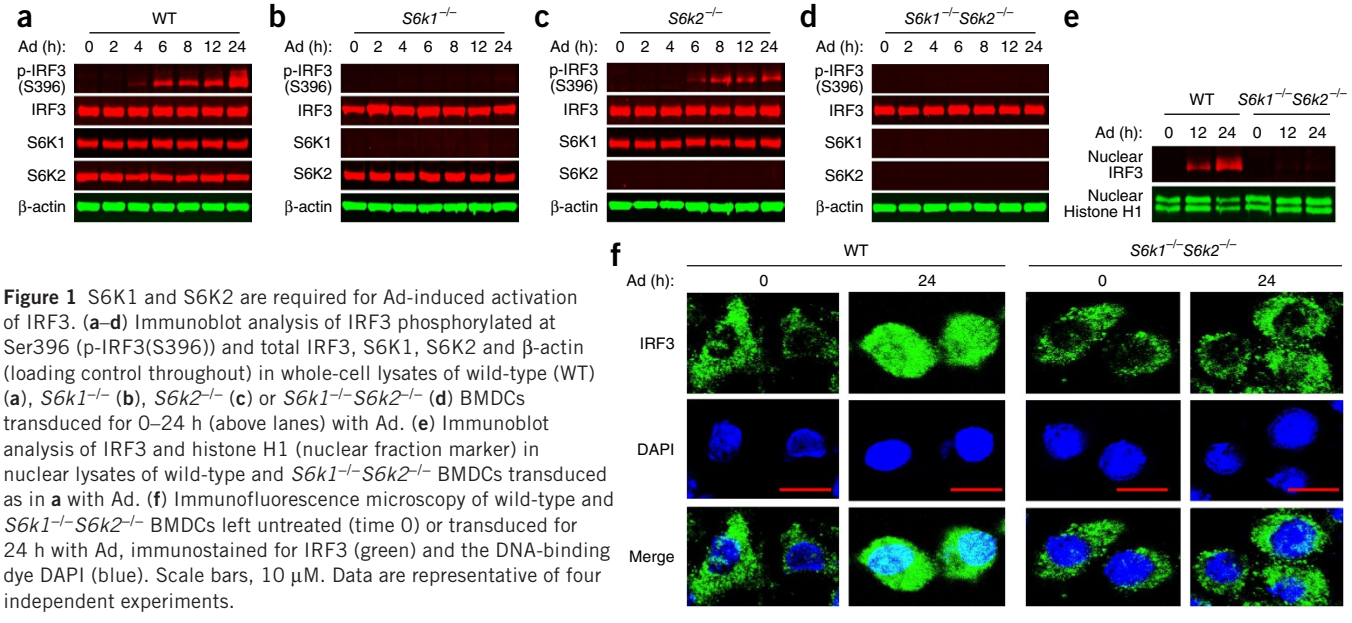

Figure 1 S6K1 and S6K2 are required for Ad-induced activation of IRF3. (**a**–**d**) Immunoblot analysis of IRF3 phosphorylated at Ser396 (p-IRF3(S396)) and total IRF3, S6K1, S6K2 and β-actin (loading control throughout) in whole-cell lysates of wild-type (WT) (**a**), *S6k1*$^{-/-}$ (**b**), *S6k2*$^{-/-}$ (**c**) or *S6k1*$^{-/-}$*S6k2*$^{-/-}$ (**d**) BMDCs transduced for 0–24 h (above lanes) with Ad. (**e**) Immunoblot analysis of IRF3 and histone H1 (nuclear fraction marker) in nuclear lysates of wild-type and *S6k1*$^{-/-}$*S6k2*$^{-/-}$ BMDCs transduced as in **a** with Ad. (**f**) Immunofluorescence microscopy of wild-type and *S6k1*$^{-/-}$*S6k2*$^{-/-}$ BMDCs left untreated (time 0) or transduced for 24 h with Ad, immunostained for IRF3 (green) and the DNA-binding dye DAPI (blue). Scale bars, 10 μM. Data are representative of four independent experiments.

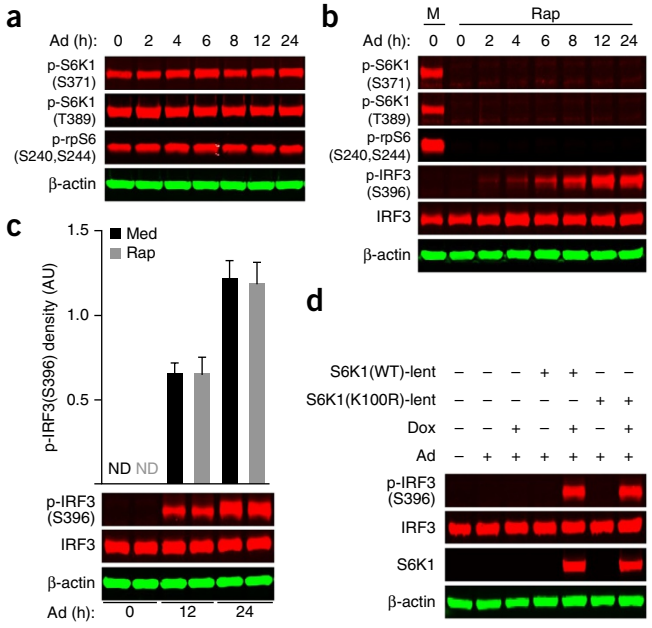

Figure 2 The regulation of Ad-induced activation of IRF3 by S6K is independent of the kinase function of S6K. (**a**) Immunoblot analysis of S6K1 phosphorylated at Ser371 (p-S6K1(S371)) or Thr389 (p-S6K1(T389)) and rpS6 phosphorylated at Ser240 and Ser244 (p-rpS6(S240,S244)) in whole-cell lysates of wild-type BMDCs transduced for 0–24 h (above lanes) with Ad. (**b**) Immunoblot analysis of p-S6K1(S371), p-S6K1(T389), p-rpS6(S240,S244), p-IRF3(S396) and total IRF3 in whole-cell lysates of wild-type BMDCs pre-treated for 2 h with medium alone (M) or rapamycin (Rap) (top) and then transduced for 0–24 h (above lanes) with Ad. (**c**) Immunoblot analysis (bottom) of p-IRF3(S396) and total IRF3 in whole-cell lysates of wild-type BMDCs pre-treated for 2 h with medium alone (Med) or rapamycin (Rap) and then transduced for 0–24 h (below lanes) with Ad; above, band density of phosphorylated IRF3 relative to that of total IRF3, in arbitrary units (AU). ND, not detected. (**d**) Immunoblot analysis of p-IRF3(S396) and total IRF3 and S6K1 in whole-cell lysates of *S6k1*$^{-/-}$*S6k2*$^{-/-}$ BMDCs left untransduced (–) or transduced (+) for 96 h with lentivirus expressing wild-type (S6K1(WT)-lent) or S6K1(K100R) (S6K1(K100R)-lent), then left uninduced (–) or induced (+) for 24 h with doxycycline (Dox) and then left uninfected (–) or infected (+) for 24 h with Ad. Data are representative of three independent experiments.

(*Irf3*$^{-/-}$) BMDCs (**Supplementary Fig. 3f**). Together these data suggested that S6K-IRF3 signaling was a crucial temporal regulator for the early-phase induction of IRF3 target genes in the cytosolic DNA pathway.

IRF3 activation does not require the kinase function of S6K

S6Ks are known to regulate various cellular events through their kinase function[16]. To ascertain whether the kinase activity of S6K was critical in Ad-triggered activation of IRF3, we first characterized the phosphorylation of S6K1 at Ser371 and Thr389 (refs. 16,25). Immunoblot analysis with antibodies specific for phosphorylation at these sites indicated that S6K1 was phosphorylated in BMDCs even in the absence of Ad transduction (**Fig. 2a**). In addition, the prototypic S6K substrate rpS6 (ribosomal protein S6)[16,25] was also constitutively phosphorylated at Ser240 and Ser244 in unstimulated BMDCs (**Fig. 2a**), which indicated that phosphorylated S6K1 signaled to its downstream target rpS6 in BMDCs at steady state.

The phosphorylation of S6K1 at Ser371 and Thr389 remained the same after the transduction of Ad as it was in non-transduced BMDCs (**Fig. 2a**). Pretreatment with the mTOR inhibitor rapamycin[16,26] for 2 h before Ad transduction abolished the phosphorylation of S6K1 and rpS6 in wild-type BMDCs (**Fig. 2b**). Despite the profound suppression of S6K1 phosphorylation, Ad-triggered IRF3 phosphorylation was not inhibited by rapamycin (**Fig. 2b,c**). Notably, we observed that lentiviral reconstitution with a kinase-inactive version of S6K1 (S6K1(K100R)) restored the Ad-induced phosphorylation of IRF3 in *S6k1*$^{-/-}$*S6k2*$^{-/-}$ BMDCs (**Fig. 2d**). These observations

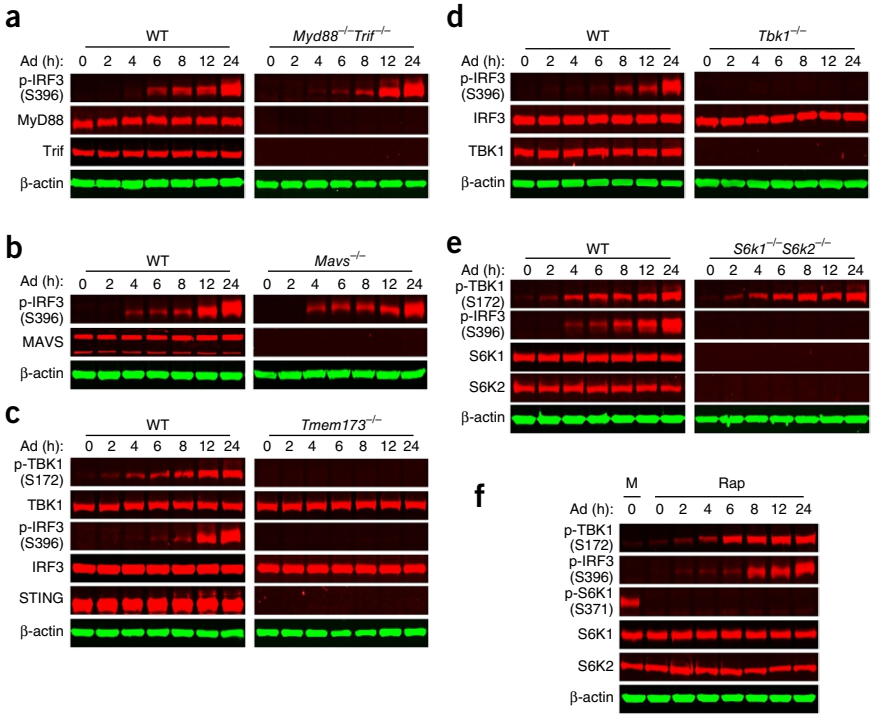

Figure 3 Ad-triggered, STING-dependent activation of TBK1 does not require S6K1 or S6K2. (**a**) Immunoblot analysis of p-IRF3(S396) and total MyD88 and TRIF in whole-cell lysates of *Myd88*$^{-/-}$*Trif*$^{-/-}$ BMDCs transduced for 0–24 h (above lanes) with Ad. (**b**) Immunoblot analysis of p-IRF3(S396) and total MAVS in whole-cell lysates of wild-type and *Mavs*$^{-/-}$ BMDCs transduced with Ad as in **a**. (**c**) Immunoblot analysis of TBK1 phosphorylated at Ser172 (p-TBK1(S172)) and total TBK1, p-IRF3(S396) and total IRF3, and total STING in whole-cell lysates of wild-type and *Tmem173*$^{-/-}$ BMDCs transduced with Ad as in **a**. (**d**) Immunoblot analysis of p-IRF3(S396) and total IRF3 and TBK1 in whole-cell lysates of wild-type and *Tbk1*$^{-/-}$ BMDCs transduced with Ad as in **a**. (**e**) Immunoblot analysis of p-TBK1(S172), p-IRF3(S396) and total S6K1 and S6K2 in whole-cell lysates of wild-type and *S6k1*$^{-/-}$*S6k2*$^{-/-}$ BMDCs transduced with Ad as in **a**. (**f**) Immunoblot analysis of p-TBK1(S172), p-IRF3(S396), p-S6K1(Ser371), and total S6K1 and S6K2 in whole-cell lysates of wild-type and *S6k1*$^{-/-}$*S6k2*$^{-/-}$ BMDCs pre-treated for 2 h with medium alone (M) or rapamycin (Rap) (top) and then transduced with Ad as in **a**. Data are representative of three independent experiments.

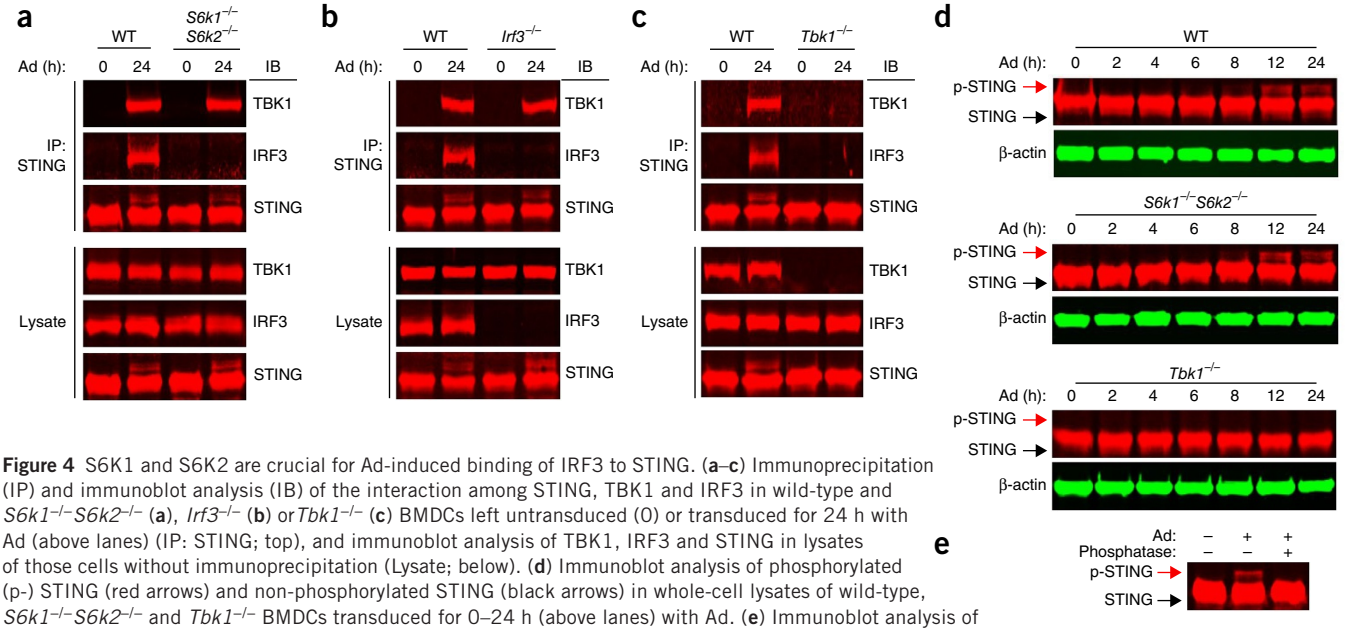

Figure 4 S6K1 and S6K2 are crucial for Ad-induced binding of IRF3 to STING. (**a**–**c**) Immunoprecipitation (IP) and immunoblot analysis (IB) of the interaction among STING, TBK1 and IRF3 in wild-type and *S6k1*$^{-/-}$*S6k2*$^{-/-}$ (**a**), *Irf3*$^{-/-}$ (**b**) or *Tbk1*$^{-/-}$ (**c**) BMDCs left untransduced (0) or transduced for 24 h with Ad (above lanes) (IP: STING; top), and immunoblot analysis of TBK1, IRF3 and STING in lysates of those cells without immunoprecipitation (Lysate; below). (**d**) Immunoblot analysis of phosphorylated (p-) STING (red arrows) and non-phosphorylated STING (black arrows) in whole-cell lysates of wild-type, *S6k1*$^{-/-}$*S6k2*$^{-/-}$ and *Tbk1*$^{-/-}$ BMDCs transduced for 0–24 h (above lanes) with Ad. (**e**) Immunoblot analysis of phosphorylated and non-phosphorylated STING (as in **d**) in whole-cell lysates of wild-type BMDCs left untransduced (–) or transduced (+) for 24 h with Ad, then left untreated (–) or treated (+) with calf intestine phosphatase. Data are representative of four independent experiments.

indicated that S6K was required for the Ad-triggered activation of IRF3, but its kinase activity was not.

Activation of TBK1 by STING does not involve S6K1 or S6K2

To define the mechanisms of S6K's action in IRF3 signaling, we carried out Ad transduction of BMDCs in which key adaptors representing distinct signaling cascades were ablated genetically. We observed that Ad-triggered IRF3 phosphorylation was unimpaired in BMDCs deficient in the adaptors MyD88 and TRIF (*Myd88*$^{-/-}$*Ticam1*$^{-/-}$; called '*Myd88*$^{-/-}$*Trif*$^{-/-}$' here) (**Fig. 3a**). Similarly, Ad-triggered phosphorylation of IRF3 in BMDCs deficient in the adaptor MAVS (*Mavs*$^{-/-}$) was intact (**Fig. 3b**). In contrast, genetic ablation of STING (*Tmem173*$^{-/-}$), an adaptor that represents the cytosolic DNA pathway[12,27], abolished Ad-induced phosphorylation of IRF3 (**Fig. 3c**), which confirmed that the cytosolic DNA–mediated, STING-dependent pathway was responsible for the Ad-induced activation of IRF3 in BMDCs.

Cellular sensing of virally presented cytosolic DNA causes STING to recruit and activate TBK1 (refs. 6,7,9). Activated TBK1 in turn phosphorylates its downstream substrate IRF3 (refs. 6,7,9). Thus, we investigated the contribution of S6K1 to the STING signalosome that links to TBK1 and IRF3. Ad induced robust phosphorylation of TBK1 at Ser172, a hallmark of TBK1 activation, in wild-type BMDCs (**Fig. 3c**). Notably, genetic deletion of STING abolished the Ad-induced phosphorylation of TBK1 (**Fig. 3c**), which correlated with the absence of IRF3 phosphorylation in TBK1-deficient (*Tbk1*$^{-/-}$) BMDCs (**Fig. 3d**). These data confirmed the conclusions that STING functioned upstream of TBK1 and that TBK1 was the key kinase responsible for Ad-triggered phosphorylation of IRF3 in BMDCs. However, despite the profound suppression of IRF3 phosphorylation in *S6k1*$^{-/-}$*S6k2*$^{-/-}$ BMDCs (**Fig. 3e**), Ad-triggered phosphorylation of TBK1 was normal in such cells (**Fig. 3e**). Consistent with that, we observed that rapamycin did not inhibit the Ad-triggered phosphorylation of TBK1 in BMDCs (**Fig. 3f**). Rapamycin inhibited only the kinase activity of S6K but did not deplete BMDCs of S6K proteins (**Fig. 3f**). As expected, rapamycin did not suppress IRF3 phosphorylation in BMDCs (**Fig. 3f**). Together these results indicated that unlike the activation of IRF3, the STING-dependent activation of TBK1 occurred independently of S6K1 and S6K2, which suggested that S6K1 and S6K2 modified the ability of activated TBK1 to phosphorylate IRF3 in the context of an Ad-triggered and STING-dependent recognition signal in BMDCs.

Requirement for S6K1 and S6K2 in the binding of IRF3 to STING

STING has a scaffold function and binds both TBK1 and IRF3 (ref. 28). To investigate if S6K influenced the IRF3-TBK1 interaction via STING, we conducted co-immunoprecipitation studies and observed that endogenous STING bound to both TBK1 and IRF3 in Ad-transduced BMDCs (**Fig. 4a**). Although genetic deletion of S6K1 and S6K2 did not impair the TBK1-STING interaction (**Fig. 4a**), the binding of IRF3 to STING was abolished in *S6k1*$^{-/-}$*S6k2*$^{-/-}$ BMDCs (**Fig. 4a**). These data suggested that S6K1 and S6K2 were required for the binding of IRF3 to the activated STING in the Ad-triggered cytosolic DNA pathway.

To extend those findings, we transduced Ad into *Irf3*$^{-/-}$ and *Tbk1*$^{-/-}$ BMDCs. STING immunoprecipitated together with TBK1 in Ad-transduced *Irf3*$^{-/-}$ BMDCs (**Fig. 4b**). In contrast, STING did not immunoprecipitate together with IRF3 in Ad-transduced *Tbk1*$^{-/-}$ BMDCs (**Fig. 4c**), which indicated that the Ad-triggered binding of TBK1 to STING occurred independently of IRF3; this would mechanistically explain the uncoupling of the activation of TBK1 and that of IRF3 (**Fig. 3e**). Phosphorylation of STING has been shown to enhance IRF3 activation[15,28]. Thus, we sought to determine whether S6K1 and S6K2 had a role in the phosphorylation of STING. In wild-type BMDCs, transduction of Ad resulted in an apparent shift in the mobility of STING in a time-dependent manner (**Fig. 4d**). Phosphatase treatment abolished the STING bands of higher molecular weight that appeared after the transduction of Ad (**Fig. 4e**), which indicated that the observed shift in the mobility of STING was due to phosphorylation. Notably, Ad-triggered shift in the STING band was unimpaired in *S6k1*$^{-/-}$*S6k2*$^{-/-}$ BMDCs (**Fig. 4d**). In contrast,

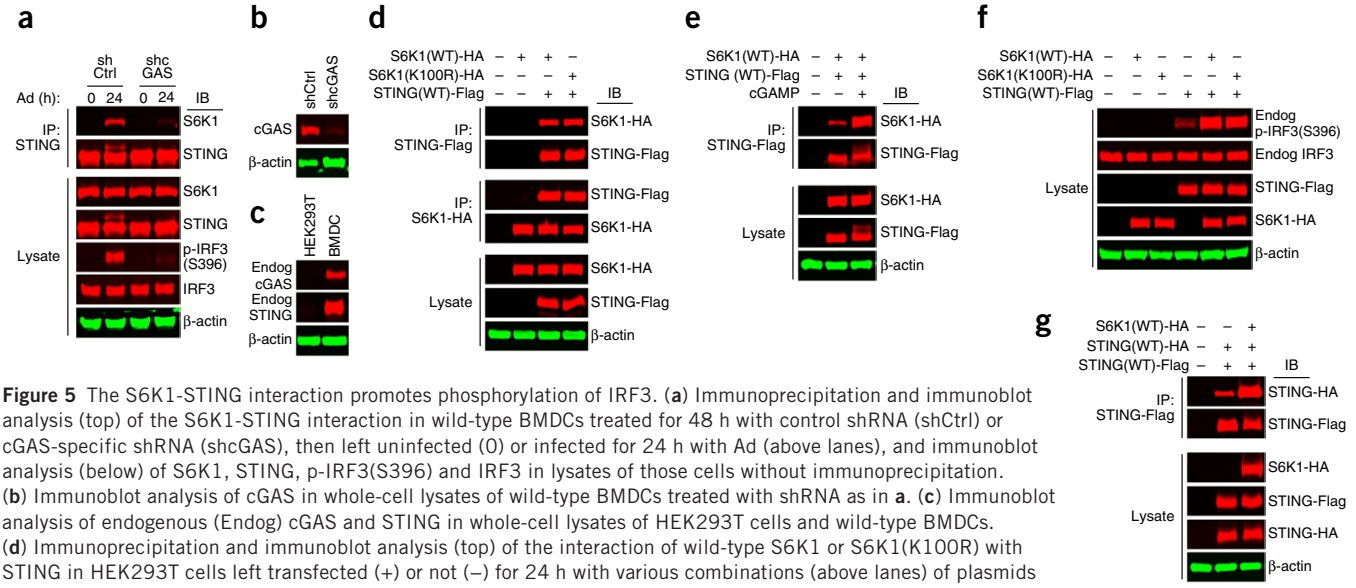

Figure 5 The S6K1-STING interaction promotes phosphorylation of IRF3. (**a**) Immunoprecipitation and immunoblot analysis (top) of the S6K1-STING interaction in wild-type BMDCs treated for 48 h with control shRNA (shCtrl) or cGAS-specific shRNA (shcGAS), then left uninfected (0) or infected for 24 h with Ad (above lanes), and immunoblot analysis (below) of S6K1, STING, p-IRF3(S396) and IRF3 in lysates of those cells without immunoprecipitation. (**b**) Immunoblot analysis of cGAS in whole-cell lysates of wild-type BMDCs treated with shRNA as in **a**. (**c**) Immunoblot analysis of endogenous (Endog) cGAS and STING in whole-cell lysates of HEK293T cells and wild-type BMDCs. (**d**) Immunoprecipitation and immunoblot analysis (top) of the interaction of wild-type S6K1 or S6K1(K100R) with STING in HEK293T cells left transfected (+) or not (–) for 24 h with various combinations (above lanes) of plasmids encoding S6K1(WT)-HA, S6K1(K100R)-HA and STING(WT)-Flag, and immunoblot analysis (below) of S6K1-HA and STING-Flag in lysates of those cells without immunoprecipitation. (**e**) Immunoprecipitation and immunoblot analysis (top) of the interaction of S6K1 and STING in HEK293T cells transfected (+) or not (–) for 24 h with plasmids encoding S6K1(WT)-HA and STING(WT)-Flag, then transfected (+) or not (–) for 6 h with 2′,3′ cGAMP, and immunoblot analysis (below) of S6K1-HA and STING-Flag in lysates of those cells without immunoprecipitation. (**f**) Immunoblot analysis of endogenous p-IRF3(S396) and total IRF3, as well as STING-Flag and S6K1-HA, in whole-cell lysates of HEK293T cells transfected (+) or not (–) for 24 h with various combinations (above lanes) of plasmids encoding S6K1(WT)-HA or S6K1(K100R)-HA and STING(WT)-Flag. (**g**) Immunoprecipitation and immunoblot analysis (top) of the interaction between STING-HA and STING-Flag in HEK293T cells transfected (+) or not (–) for 24 h with plasmids encoding STING(WT)-HA and STING(WT)-Flag with or without plasmid encoding S6K1(WT)-HA, and immunoblot analysis (below) of S6K1-HA, STING-Flag and STING-HA in lysates of those cells without immunoprecipitation. Data are representative of three independent experiments.

Ad was unable to elicit this shift in *Tbk1*$^{-/-}$ BMDCs (**Fig. 4d**), which demonstrated that the Ad-triggered phosphorylation of STING was TBK1 dependent. Notably, we observed that although infection with VSV resulted in substantial phosphorylation of IRF3, it did not cause any discernible shift in the mobility of STING (**Supplementary Fig. 4a**). This was consistent with the finding that MAVS was required for VSV-induced activation of IRF3 in BMDCs (**Supplementary Fig. 4a**), which emphasized that the activation of STING constitutes a hallmark for cytosolic DNA–mediated signaling[12,27]. Collectively, these results suggested an important role for S6K in facilitating the binding of IRF3 to cytosolic DNA–activated STING.

S6K1 interacts with STING to promote IRF3 phosphorylation

The requirement for S6K1 and S6K2, particularly S6K1, for the binding of IRF3 to activated STING suggested an interaction between S6K1 and STING in Ad-transduced BMDCs. To explore this possibility, we performed endogenous co-immunoprecipitation assays. While S6K1 and STING did not associate in mock-infected BMDCs, Ad induced the interaction of endogenous S6K1 with STING in BMDCs (**Fig. 5a**). Of note, when the cytosolic DNA sensor cGAS was silenced through the use of cGAS-specific short hairpin RNA (shRNA) in BMDCs (**Fig. 5a**,**b**), the endogenous S6K1-STING interaction was reduced (**Fig. 5a**) and phosphorylation of IRF3 was inhibited (**Fig. 5a**). In contrast, lipopolysaccharide or VSV did not induce the co-immunoprecipitation of S6K1 and STING in BMDCs (**Supplementary Fig. 4b**) under conditions in which IRF3 was potently phosphorylated (**Supplementary Fig. 4b**). Collectively, these results indicated that the S6K-STING interaction occurred only in the cytosolic DNA–cGAS–STING pathway to promote the phosphorylation of IRF3.

Next we transfected S6K1 and STING expression plasmids into HEK293T cells, which are human embryonic kidney cells widely used as transfection hosts that lack endogenous cGAS and STING[6,29] (**Fig. 5c**). Co-transfection resulted in an association between hemagglutinin (HA)-tagged mouse S6K1 (S6K1-HA) and Flag-tagged mouse STING (STING-Flag) (**Fig. 5d**). Notably, HA-tagged kinase-inactive S6K1 (S6K1(K100R)-HA)[30] bound to Flag-tagged wild-type STING (STING(WT)-Flag) in a manner similar to that of HA-tagged wild-type S6K1 (S6K1(WT)-HA) (**Fig. 5d**), which indicated that the S6K1-STING interaction in mammalian cells did not require the kinase function of S6K1. Next we investigated the influence of STING activation on the S6K1-STING interaction through the use of the STING activator cGAMP[8,24] in HEK293T cells, which do not express endogenous cGAS (**Fig. 5c**) and do not produce endogenous cGAMP[6]. Because ectopically expressed STING is reported to be auto-activated in a ligand-independent manner[29,31], we transfected HEK293T cells with a 'pre-titrated' amount of plasmid encoding STING(WT)-Flag together with plasmid encoding S6K1(WT)-HA such that STING-Flag remained responsive, and treated the co-transfected HEK293T cells with cGAMP. We observed that cGAMP increased the interaction of S6K1(WT)-HA and STING(WT)-Flag in HEK293T cells (**Fig. 5e**). To evaluate the physiological relevance of this interaction, we transfected HEK293T cells with a 'pre-tested' amount of plasmid encoding STING(WT)-Flag such that STING-Flag induced only minimal phosphorylation of IFR3 (**Fig. 5f**). Co-transfection of plasmid encoding STING(WT)-Flag together with plasmid encoding S6K1(WT)-HA or S6K1(K100R)-HA similarly augmented the STING-Flag–dependent phosphorylation of endogenous IRF3 in HEK293T cells (**Fig. 5f**).

Next we explored whether S6K1 affected the dimerization or oligomerization of STING, as this is a key process for signal propagation in signaling via the innate immune system[14,27,28]. In HEK293T cells co-transfected with plasmids encoding HA-tagged wild-type STING (STING(WT)-HA) and STING(WT)-Flag, STING existed partially as a dimer (**Fig. 5g**). However, the fraction of STING dimer

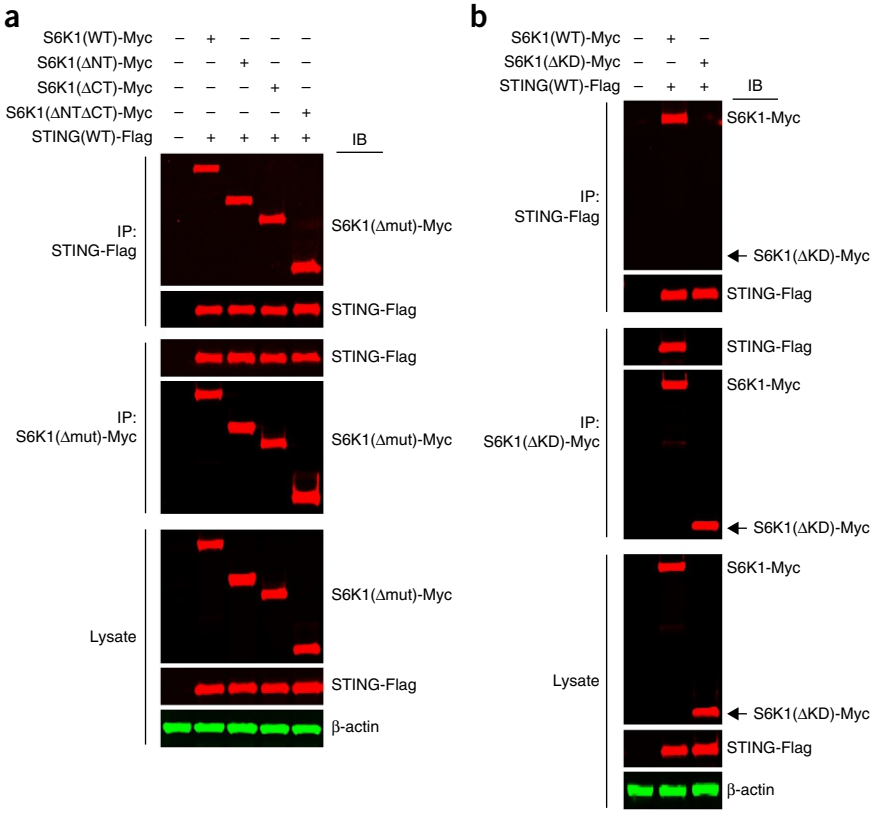

Figure 6 The kinase domain of S6K1, but neither its N terminus or C terminus, is involved in mediating the interaction of S6K1 with STING. (**a**) Immunoprecipitation and immunoblot analysis (top) of the interaction between STING-Flag and Myc-tagged S6K1 truncation mutants (S6K1 (Δmut)-Myc) in HEK293T cells transfected (+) or not (–) for 24 h with various combinations (above lanes) of plasmids encoding STING(WT)-Flag and Myc-tagged wild-type S6K1 (S6K1(WT)-Myc) or S6K1 truncation mutants lacking the N terminus (S6K1 (ΔNT)-Myc) or C terminus (S6K1(ΔCT)-Myc) or both (S6K1(ΔNTΔCT)-Myc), and immunoblot analysis (below) of S6K1(Δmut)-Myc and STING-Flag in lysates of those cells without immunoprecipitation. (**b**) Immunoprecipitation and immunoblot analysis (top) of the interaction between STING-Flag and Myc-tagged wild-type S6K1 or mutant S6K1 with deletion of its kinase domain (S6K1(ΔKD)) in HEK293T cells transfected (+) or not (–) for 24 h with various combinations (above lanes) of plasmid encoding STING(WT)-Flag with plasmid encoding Myc-tagged wild-type S6K1 (S6K1(WT)-Myc) or S6K1(ΔKD) (S6K1(ΔKD)-Myc), and immunoblot analysis (below) of Myc-tagged wild-type S6K1 or S6K1(ΔKD) and STING-Flag in lysates of those cells without immunoprecipitation. Data are representative of three independent experiments.

was increased substantially when cells were co-transfected with plasmid encoding S6K1(WT)-HA (**Fig. 5g**), which suggested that the S6K1-STING interaction augmented the formation or stabilization of STING dimers or oligomers.

The N- and C-terminal regions of S6K1 are known to regulate its activity[16,32]. To determine whether these regions were involved in the S6K1-STING interaction, we transfected plasmid encoding STING(WT)-Flag into HEK293T cells together with plasmid encoding Myc-tagged wild-type S6K1 or various truncation mutants of S6K1. Truncation of the S6K1 N terminus had no effect on the interaction of Myc-tagged S6K1 and STING(WT)-Flag (**Fig. 6a**). Notably, deletion of the S6K1 C terminus did not exert an inhibitory effect either (**Fig. 6a**). The C termini of signaling proteins are often involved in protein-protein interactions[15,28,33]. Thus, to further confirm the lack of involvement of the S6K1 C terminus in the S6K1-STING interaction, we used a construct that expressed only the C terminus of S6K1. The S6K1 C terminus was unable to associate with STING in HEK293T cells (**Supplementary Fig. 5a**), which demonstrated that the regulatory domains of S6K1 required for canonical mTOR-S6K1 signaling were not required for the binding of S6K1 to STING. In contrast, mutant S6K1 with deletion of its kinase domain abolished the S6K1-STING interaction in HEK293T cells (**Fig. 6b**).

Next we determined which S6K1 domain(s) was (were) involved in augmenting the STING-induced phosphorylation of IRF3, as STING is the key structure for anchoring IRF3 for its phosphorylation by TBK1 (refs. 28,33). Following co-transfection of HEK293T cells with plasmids encoding various Myc-tagged wild-type or mutant S6K1 together with plasmid encoding STING(WT)-Flag, Myc-tagged wild-type S6K1 substantially enhanced the STING-Flag–dependent phosphorylation of IRF3 (**Supplementary Fig. 5b**). Notably, this enhancement of IRF3 phosphorylation by S6K1 remained unchanged when plasmid encoding S6K1 lacking its N terminus or its C terminus or both was transfected together with plasmid encoding STING(WT)-Flag (**Supplementary Fig. 5b**). In contrast, S6K1 with deletion of its kinase domain was unable to promote the STING-dependent phosphorylation of IRF3 (**Supplementary Fig. 5b**). Collectively, these data identified S6K as an additional binding partner of STING for the promotion of IRF3 phosphorylation.

Formation of a tripartite S6K1-STING-TBK1 complex

To further investigate how TBK1 modulated the S6K1-STING interaction, we silenced expression of the gene encoding TBK1 in HEK293T cells through the use of TBK1-specific shRNA (**Fig. 7a**). Silencing of the gene encoding TBK1 markedly inhibited the interaction of S6K1(WT)-HA and STING(WT)-Flag (**Fig. 7b**), which indicated a pivotal role for TBK1 in the S6K1-STING association. To address whether S6K1 and TBK1 interacted directly, we took advantage of the lack of endogenous STING in HEK293T cells[6] and co-transfected plasmids encoding S6K1(WT)-HA and Flag-tagged wild-type TBK1 (TBK1(WT)-Flag) into these cells. We did not observe an appreciable direct interaction between S6K1(WT)-HA and TBK1(WT)-Flag in the absence of endogenous STING (**Fig. 7c**), which suggested that TBK1 might modify STING activity by unveiling a docking site on STING for S6K1.

To test our hypothesis, we co-transfected plasmids encoding S6K1(WT)-HA and STING(WT)-Flag into HEK293T cells with or without plasmid encoding Flag-tagged wild-type TBK1 (TBK1(WT)-Flag) or kinase-inactive TBK1 mutant (TBK1(K38A)-Flag)[34]. TBK1(WT)-Flag and TBK1(K38A)-Flag were expressed at similar levels (**Fig. 7d**). Notably, co-transfection of plasmid encoding TBK1(WT)-Flag resulted in a shift to STING bands of higher molecular weight, but co-transfection of plasmid encoding TBK1(K38A)-Flag did not (**Fig. 7d**), and the shifted bands disappeared after treatment

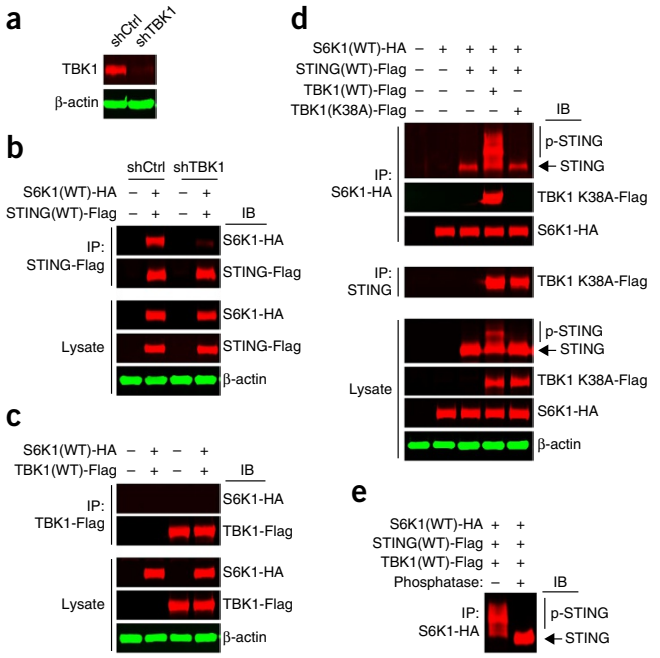

Figure 7 S6K1 interacts with STING and TBK1 to form a tripartite complex. (**a**) Immunoblot analysis of TBK1 in HEK293T cells treated with control shRNA (shCtrl) or TBK1-specific shRNA (shTBK1). (**b**) Immunoprecipitation and immunoblot analysis (top) of the interaction between S6K1 and STING in HEK293T cells treated with shRNA as in **a** and transfected (+) or not (–) with plasmids encoding S6K1(WT)-HA and STING(WT)-Flag, and immunoblot analysis (below) of S6K1-HA and STING-Flag in lysates of those cells without immunoprecipitation. (**c**) Immunoprecipitation and immunoblot analysis (top) of the interaction between S6K1 and TBK1 in HEK293T cells transfected (+) or not (–) with plasmids encoding S6K1(WT)-HA and TBK1(WT)-Flag, and immunoblot analysis (below) of S6K1-HA and TBK1-Flag in lysates of those cells without immunoprecipitation. (**d**) Immunoprecipitation and immunoblot analysis of the interactions among S6K1, STING and wild-type TBK1 or TBK1(K38A) in HEK293T cells transfected for 24 h with various combinations (above lanes) of plasmids encoding S6K1(WT)-HA, STING(WT)-Flag and TBK1(WT)-Flag or TBK1(K38A)-Flag, and immunoblot analysis (below) of phosphorylated STING (vertical line), non-phosphorylated STING (arrow), S6K1-HA and TBK1-Flag in lysates of those cells without immunoprecipitation. (**e**) Immunoblot analysis of phosphorylated and non-phosphorylated STING (as in **d**) in immunoprecipitates precipitated with antibody to S6K1-HA from whole-cell lysates of HEK293T cells triply transfected for 24 h with plasmids encoding S6K1(WT)-HA, STING(WT)-Flag and TBK1(WT)-Flag and treated with calf intestine phosphatase (+) or not (–). Data are representative of four independent experiments.

with phosphatase (data not shown), indicative of TBK1-dependent phosphorylation of STING. Notably, when cells were co-transfected with plasmid encoding TBK1(WT)-Flag, the STING(WT)-Flag precipitated by S6K1(WT)-HA seemed to be largely phosphorylated, as indicated by its slower mobility (**Fig. 7d**) and results obtained by treatment with phosphatase (**Fig. 7e**). In contrast, no STING with a shift in mobility was precipitated by S6K1(WT)-HA in the presence of TBK1(K38A)-Flag (**Fig. 7d**). The faster migrating band of STING precipitated by S6K1(WT)-HA in the presence of TBK1(K38A)-Flag (**Fig. 7d**) could have been attributed to the endogenous TBK1, as that band was further diminished in cells in which TBK1 was knocked down and that were triply transfected with plasmids encoding S6K1(WT)-HA, STING(WT)-Flag and TBK1(K38A)-Flag (data not shown).

Of note, S6K1(WT)-HA also precipitated together with TBK1(WT)-Flag but not with TBK1(K38A)-Flag (**Fig. 7d**) even though both bound to STING (**Fig. 7d**); this indicated that the binding of TBK1 to STING alone might not have been sufficient for promoting an interaction event between S6K1 and STING and suggested an important role for TBK1-mediated phosphorylation of STING in facilitating the S6K1-STING interaction. To further confirm that hypothesis, we found that isolated recombinant TBK1(WT)-Flag caused phosphorylation of isolated STING(WT)-Flag in an *in vitro* kinase assay (as demonstrated by slower mobility), but isolated recombinant S6K1(WT)-HA did not (**Supplementary Fig. 6**). Isolated S6K1(WT)-HA precipitated together with both isolated STING(WT)-Flag and TBK1(WT)-Flag following the kinase reaction (**Supplementary Fig. 6**), Collectively, these results further demonstrated that S6K1 was able to interact directly with phosphorylated STING and form a S6K1-STING-TBK1 tripartite complex in mammalian cells.

Requirement for S6K-IRF3 signaling in *in vivo* antiviral immunity

To assess the physiological relevance of S6K in Ad-induced IRF3 signaling in BMDCs, we used Ad-transduced DC–based vaccination as an *in vivo* system. We transduced wild-type, $S6k1^{-/-}S6k2^{-/-}$ and $Irf3^{-/-}$ BMDCs with either an empty Ad vector or Ad vector encoding the chicken ovalbumin peptide SIINFEKL (Ad-OVA), as a model foreign antigen, and injected these transduced BMDCs into the footpads of wild-type recipient mice. We observed that the transfer of Ad-OVA–transduced $S6k1^{-/-}S6k2^{-/-}$ or $Irf3^{-/-}$ BMDCs resulted in significantly impaired OVA-specific $CD8^+$ T cell responses compared with those of mice inoculated with Ad-OVA–transduced wild-type BMDCs (**Fig. 8a**). Subsequent challenge of the BMDC-vaccinated mice with a single intraperitoneal injection of recombinant vaccinia virus expressing OVA (VV-OVA) showed that the mice vaccinated with Ad-OVA–transduced $S6k1^{-/-}S6k2^{-/-}$ or $Irf3^{-/-}$ BMDCs failed to control infection with vaccinia virus (**Fig. 8b**).

S6Ks are known for their role in the translation of mRNA[35]. Notably, $S6k1^{-/-}S6k2^{-/-}$ BMDCs showed expression of Ad transgene–encoded antigens similar to that of wild-type BMDCs (**Supplementary Fig. 7a**,**b**), which indicated that $S6k1^{-/-}S6k2^{-/-}$ BMDCs were not impaired in their ability to induce T cell responses due to global defects in protein expression. Similarly, $S6k1^{-/-}S6k2^{-/-}$ BMDCs exhibited a level of SIINFEKL peptide presentation (via $H\text{-}2K^b$) similar to that of $Irf3^{-/-}$ and wild-type BMDCs (**Supplementary Fig. 7c**). In addition, $S6k1^{-/-}S6k2^{-/-}$ BMDCs had an ability to migrate to draining lymph nodes similar to the migration ability of $Irf3^{-/-}$ and wild-type BMDCs (**Supplementary Fig. 7d**,**e**), and in those lymph nodes, they displayed surface expression of the integrin CD11c similar to that of $Irf3^{-/-}$ and wild-type BMDCs (data not shown). Collectively, these data indicated that S6K-IRF3 signaling in the donor BMDCs was important for the induction of optimal antigen-specific T cell responses by DNA vector–transduced DCs in the recipient hosts.

Furthermore, the innate antiviral response to HSV-1 is STING dependent[12]. This virus can cause productive infection in mice when transmitted via the intravaginal route[12]. We observed that HSV-1 replication was markedly increased in the vaginal tract of both $S6k1^{-/-}S6k2^{-/-}$ mice and $Irf3^{-/-}$ mice compared with its replication in wild-type mice (**Fig. 8c**), which indicated that infection of the vaginal mucosa with HSV-1 was also restricted by S6K-dependent IRF3 signaling. Together these findings suggested that S6K-IRF3 signaling is an important defense component in the host immune network.

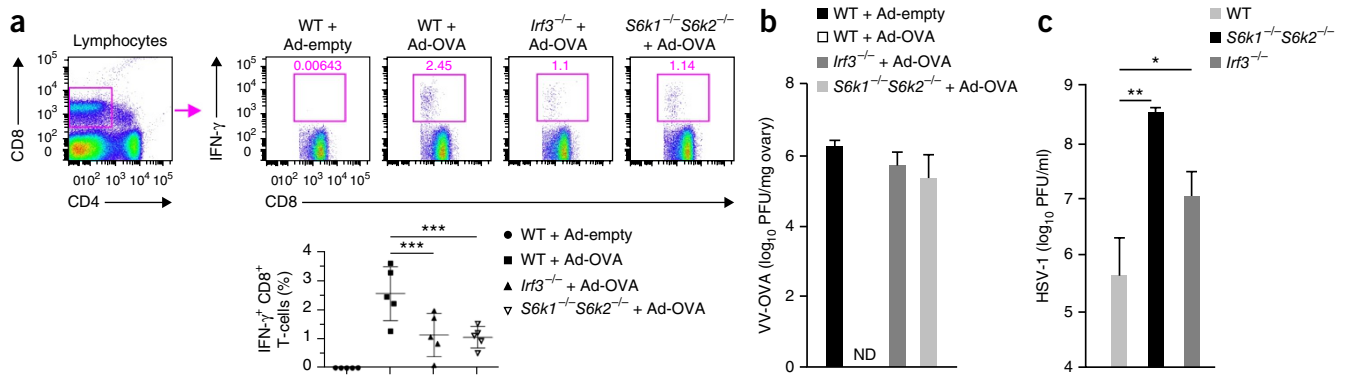

Figure 8 Disruption of DNA virus–induced S6K-IRF3 signaling in donor BMDCs impairs the induction of T cell responses in the recipient host. (**a**) Flow cytometry of lymphocytes from C57BL/6 mice (far left) and of OVA-specific T cells (right) in wild-type recipient mice vaccinated with wild-type, *S6k1*$^{-/-}$*S6k2*$^{-/-}$ or *Irf3*$^{-/-}$ BMDCs transduced with empty Ad vector (Ad-empty) or Ad-OVA (above plots). Numbers above outlined areas (right) indicate percent interferon-γ-positive (IFN-γ^{+}) CD8^{+} T cells. Below, summary of the frequency of IFN-γ^{+}CD8^{+} T cells. Each symbol (below) represents an individual mouse; small horizontal lines indicate the mean (± s.d.). (**b**) Plaque assay of VV-OVA in the ovaries of wild-type C57BL/6 host mice ($n = 5$ per group) vaccinated with BMDCs as in **a** (key) and challenged by infection with VV-OVA. PFU, plaque-forming units. (**c**) Plaque assay of HSV-1 in the vaginal washes of wild-type mice ($n = 8$), *S6k1*$^{-/-}$*S6k2*$^{-/-}$ mice ($n = 3$) and *Irf3*$^{-/-}$ mice ($n = 5$) infected intravaginally for 48 h with HSV-1. $^{*}P < 0.05$, $^{**}P < 0.01$ and $^{***}P < 0.001$ (one way analysis of variance). Data are representative of three (**a**,**b**) or two (**c**) independent experiments (mean and s.d. in **b**,**c**).

DISCUSSION

S6Ks are known to have extensive roles in important cellular processes such as mitochondrial metabolism, cell-cycle progress and ribosome biogenesis[16]. In this study, we found that S6K1 and S6K2 were required for DNA virus–triggered activation of IRF3 in BMDCs. We have provided evidence that S6K1 associated physically with activated STING and formed a tripartite S6K1-STING-TBK1 signaling complex. We further demonstrated that S6K-mediated IRF3 signaling contributed to the early-phase expression of IRF3 target genes and the induction of robust T cell responses and mucosal antiviral defense. Thus, our report has revealed a crucial function for S6K1 and S6K2 in regulating the cytosolic DNA–cGAS–STING pathway to activate IRF3.

S6Ks are serine-threonine kinases whose function is subject to rapamycin inhibition[16]. Published reports have shown that treatment with rapamycin substantially suppresses the induction of interferons and proinflammatory cytokines in a variety of cell types, including plasmacytoid DCs, glioma cells and keratinocytes[17–19], which suggests that the kinase activity of S6Ks is required for regulating these signaling processes. Here we found that S6K-dependent activation of IRF3 was resistant to inhibition via rapamycin in BMDCs following transduction of Ad. In addition, a kinase-inactive version of S6K1 restored the Ad-induced phosphorylation of IRF3 in *S6k1*$^{-/-}$*S6k2*$^{-/-}$ BMDCs to a level similar to that achieved by wild-type S6K1. Thus, the kinase-independent role of S6K1 and S6K2 in the activation of IRF3 provides an example of a context-specific switch in the regulatory roles of S6Ks. Of note, we did not observe any difference between wild-type BMDCs and *S6k1*$^{-/-}$*S6k2*$^{-/-}$ BMDCs in their expression of the related endogenous signaling proteins STING, TBK1 or IRF3. Moreover, we confirmed that DNA virus–mediated transgene products and antigen presentation were not inhibited in *S6k1*$^{-/-}$*S6k2*$^{-/-}$ BMDCs. These observations support the proposal that S6K protein, but not its kinase function, might directly modulate innate antiviral immunity as a result of its being a regulator of IRF3 signaling.

The activation of IRF3 is a key effector event upon which diverse regulatory signals converge in a context-specific way. On the basis of our molecular interaction data, we suggest the following model for S6K1-promoted activation of IRF3 in the cytosolic DNA–cGAS–STING pathway: upon being activated by cGAS-cGAMP, STING recruits TBK1 to form a STING-TBK1 signaling complex. This event occurs independently of S6Ks and IRF3. Subsequently, S6K1 interacts with phosphorylated STING to form a tripartite S6K1-STING-TBK1 signaling complex. Because the kinase-inactive S6K1 mutant interacted with STING in a way similar to the interaction of wild-type S6K1 with STING, our working model further suggests that independently of its kinase function, S6K1 acts as an 'auxiliary adaptor' or 'scaffold' in promoting the binding of IRF3 to the STING-TBK1 complex to facilitate the TBK1-mediated phosphorylation of IRF3.

Phosphorylation of STING by TBK1 has been shown to have an essential role in recruiting IRF3 (ref. 33). Here we found that TBK1-mediated phosphorylation of STING was crucial for the promotion of a tri-molecular S6K1-STING-TBK1 interaction, particularly in intact cells, which was required for the propagation of IRF3 signal transduction. Thus, we hypothesize that the phosphorylation site(s) on STING targeted by TBK1 used for the recruitment of IRF3 might also be involved in the S6K1-STING interaction. This hypothesis awaits substantiation in future studies.

Upon being activated by ligands in the cytosol, STING triggers both NF-κB signaling cascades and IRF3 signaling cascades[6,7,9,24]. Transduction of Ad promoted the phosphorylation of both IRF3 and NF-κB in BMDCs. However, in contrast to the phosphorylation of IRF3, the Ad-elicited phosphorylation of NF-κB was not S6K dependent in BMDCs (data not shown). This observation demonstrates the specificity of S6Ks as cellular signaling molecules.

DNA virus–transduced DC–based vaccines hold promise for the immunotherapy of cancer as well as of certain viral diseases[36]. We observed that Ad-transduced donor BMDCs required S6K-dependent IRF3 signaling to achieve optimal T cell responses in recipient hosts. This finding not only demonstrates the utility of understanding the signaling pathways of the innate immune system in virus-transduced DCs but also provides a rationale for exploring the manipulation of virus-transduced DCs *ex vivo* for the desired outcome of DC-based vaccines *in vivo*. Notably, the response to HSV-1, another DNA virus that induces a STING-dependent antiviral response[12], also depended on S6K-dependent IRF3 signaling. In the absence of S6K1 and S6K2, this virus exhibited increased replication in the mucosa.

IRF3 is a key transcription factor that mediates an array of pivotal immune processes[20,21]. Congruently, a sophisticated regulatory mechanism for the activation of IRF3 might be evolutionarily advantageous, as it would offer the host possible context-specific regulation so that a given response could be initiated in a timely way, finely tuned and properly terminated. Our discovery of S6K1 and S6K2 as crucial regulators of IRF3 provides new insight into the IRF3 signaling network, particularly in its linkage to the STING-TBK1 signaling complex, a key signalosome in cellular innate immunological responses.

METHODS

Methods and any associated references are available in the online version of the paper.

Note: Any Supplementary Information and Source Data files are available in the online version of the paper.

ACKNOWLEDGMENTS

We thank the other members of the McMaster Immunology Research Centre; N. Kazhdan, S. Collins, D. Cummings and C. Shao for technical help; M. Nolland and J. Govero for preparing wild-type and mutant mouse bones; K. McCoy (University of Bern) for *Myd88*$^{-/-}$*Trif*$^{-/-}$ mice; V. Fensterl (Cleveland Clinic) and G. Sen (Cleveland Clinic) for antibody to IFIT3; X. Feng (McMaster University) for Ad-OVA and VV-OVA; M. Orr-Asman (University of Cincinnati) and C. Mercer (University of Cincinnati) for plasmids encoding S6K1; and R. Lin (McGill University) for plasmids encoding TBK1. Supported by the Cancer Research Society/Steven E. Drabin Research Fund (T.A.), Terry Fox Foundation (B.D.L.) and the Canadian Institutes of Health Research (Y.W. and the McMaster Immunology Research Centre).

AUTHOR CONTRIBUTIONS

F.W., Y.W. and B.D.L. conceived of and designed the study and wrote the paper; F.W. did most of the work; T.A. was involved in initiating the collaboration and experimental design, prepared S6K-deficient mouse bones, and made shRNAs and various expression plasmids; K.J.S. secured and prepared various mutant mouse bones; K.S. made pcDNA3 plasmids encoding STING and S6K1; J.G.P. performed *in vivo* immunization, T cell flow cytometry and VV-OVA challenge; M.J.A. prepared plasmids; T.A., H.-D.H. and B.D.F. made plasmids encoding mutant S6K1 and prepared lentivirus expressing S6K1(K100R); C.Z. conducted genotyping of S6K-deficient mice; L.C. conducted flow cytometry of BMDCs and lymph node cells labeled with the cytosolic dye CFSE; Z.R. conducted HSV-1 mouse experiments; A.H., E.S.Y.C. and C.T. prepared BMDCs and performed gel electrophoresis during the initial stage of the project; M.S.S. prepared *Mavs*$^{-/-}$ mouse bones; Z.J. prepared *Tbk1*$^{-/-}$ mouse bones and cells; A.A.A., K.M. and N.S. provided experimental materials and work support; G.T., S.C.K., M.G. and K.A.F. provided experimental materials; and M.S.D. provided experimental materials and edited the manuscript.

COMPETING FINANCIAL INTERESTS

The authors declare no competing financial interests.

1. Hornung, V. & Latz, E. Intracellular DNA recognition. *Nat. Rev. Immunol.* **10**, 123–130 (2010).
2. Rathinam, V.A. & Fitzgerald, K.A. Cytosolic surveillance and antiviral immunity. *Curr. Opin. Virol.* **1**, 455–462 (2011).
3. Barnes, E. *et al.* Novel adenovirus-based vaccines induce broad and sustained T cell responses to HCV in man. *Sci. Transl. Med.* **4**, 115ra1 (2012).
4. Nociari, M., Ocheretina, O., Murphy, M. & Falck-Pedersen, E. Adenovirus induction of IRF3 occurs through a binary trigger targeting Jun N-terminal kinase and TBK1 kinase cascades and type I interferon autocrine signaling. *J. Virol.* **83**, 4081–4091 (2009).
5. Stein, S.C. & Falck-Pedersen, E. Sensing adenovirus infection: activation of interferon regulatory factor 3 in RAW 264.7 cells. *J. Virol.* **86**, 4527–4537 (2012).
6. Sun, L., Wu, J., Du, F., Chen, X. & Chen, Z.J. Cyclic GMP-AMP synthase is a cytosolic DNA sensor that activates the type I interferon pathway. *Science* **339**, 786–791 (2013).
7. Wu, J. *et al.* Cyclic GMP-AMP is an endogenous second messenger in innate immune signaling by cytosolic DNA. *Science* **339**, 826–830 (2013).
8. Ablasser, A. *et al.* cGAS produces a 2′-5′-linked cyclic dinucleotide second messenger that activates STING. *Nature* **498**, 380–384 (2013).
9. Gao, P. *et al.* Cyclic [G(2′,5′)pA(3′,5′)p] is the metazoan second messenger produced by DNA-activated cyclic GMP-AMP synthase. *Cell* **153**, 1094–1107 (2013).
10. Ishikawa, H. & Barber, G.N. STING is an endoplasmic reticulum adaptor that facilitates innate immune signalling. *Nature* **455**, 674–678 (2008).
11. Ishikawa, H. & Barber, G.N. The STING pathway and regulation of innate immune signaling in response to DNA pathogens. *Cell. Mol. Life Sci.* **68**, 1157–1165 (2011).
12. Ishikawa, H., Ma, Z. & Barber, G.N. STING regulates intracellular DNA-mediated, type I interferon-dependent innate immunity. *Nature* **461**, 788–792 (2009).
13. Jin, L. *et al.* MPYS, a novel membrane tetraspanner, is associated with major histocompatibility complex class II and mediates transduction of apoptotic signals. *Mol. Cell. Biol.* **28**, 5014–5026 (2008).
14. Sun, W. *et al.* ERIS, an endoplasmic reticulum IFN stimulator, activates innate immune signaling through dimerization. *Proc. Natl. Acad. Sci. USA* **106**, 8653–8658 (2009).
15. Zhong, B. *et al.* The adaptor protein MITA links virus-sensing receptors to IRF3 transcription factor activation. *Immunity* **29**, 538–550 (2008).
16. Fenton, T.R. & Gout, I.T. Functions and regulation of the 70kDa ribosomal S6 kinases. *Int. J. Biochem. Cell Biol.* **43**, 47–59 (2011).
17. Alain, T. *et al.* Vesicular stomatitis virus oncolysis is potentiated by impairing mTORC1-dependent type I IFN production. *Proc. Natl. Acad. Sci. USA* **107**, 1576–1581 (2010).
18. Cao, W. *et al.* Toll-like receptor-mediated induction of type I interferon in plasmacytoid dendritic cells requires the rapamycin-sensitive PI(3)K-mTOR-p70S6K pathway. *Nat. Immunol.* **9**, 1157–1164 (2008).
19. Zhao, J. *et al.* Mammalian target of rapamycin (mTOR) regulates TLR3 induced cytokines in human oral keratinocytes. *Mol. Immunol.* **48**, 294–304 (2010).
20. Honda, K. & Taniguchi, T. IRFs: master regulators of signalling by Toll-like receptors and cytosolic pattern-recognition receptors. *Nat. Rev. Immunol.* **6**, 644–658 (2006).
21. Ysebrant de Lendonck, L., Martinet, V. & Goriely, S. Interferon regulatory factor 3 in adaptive immune responses. *Cell. Mol. Life Sci.* **71**, 3873–3883 (2014).
22. Mohr, I. & Sonenberg, N. Host translation at the nexus of infection and immunity. *Cell Host Microbe* **12**, 470–483 (2012).
23. Loo, Y.M. & Gale, M. Jr. Immune signaling by RIG-I-like receptors. *Immunity* **34**, 680–692 (2011).
24. Gao, P. *et al.* Structure-function analysis of STING activation by c[G(2′,5′)pA(3′,5′)p] and targeting by antiviral DMXAA. *Cell* **154**, 748–762 (2013).
25. Dann, S.G., Selvaraj, A. & Thomas, G. mTOR Complex1-S6K1 signaling: at the crossroads of obesity, diabetes and cancer. *Trends Mol. Med.* **13**, 252–259 (2007).
26. Soliman, G.A. The mammalian target of rapamycin signaling network and gene regulation. *Curr. Opin. Lipidol.* **16**, 317–323 (2005).
27. Burdette, D.L. & Vance, R.E. STING and the innate immune response to nucleic acids in the cytosol. *Nat. Immunol.* **14**, 19–26 (2013).
28. Tanaka, Y. & Chen, Z.J. STING specifies IRF3 phosphorylation by TBK1 in the cytosolic DNA signaling pathway. *Sci. Signal.* **5**, ra20 (2012).
29. Burdette, D.L. *et al.* STING is a direct innate immune sensor of cyclic di-GMP. *Nature* **478**, 515–518 (2011).
30. Cheatham, L., Monfar, M., Chou, M.M. & Blenis, J. Structural and functional analysis of pp70S6k. *Proc. Natl. Acad. Sci. USA* **92**, 11696–11700 (1995).
31. Diner, E.J. *et al.* The innate immune DNA sensor cGAS produces a noncanonical cyclic dinucleotide that activates human STING. *Cell Rep.* **3**, 1355–1361 (2013).
32. Schalm, S.S. & Blenis, J. Identification of a conserved motif required for mTOR signaling. *Curr. Biol.* **12**, 632–639 (2002).
33. Liu, S. *et al.* Phosphorylation of innate immune adaptor proteins MAVS, STING, and TRIF induces IRF3 activation. *Science* **347**, aaa2630 (2015).
34. Fitzgerald, K.A. *et al.* IKKε and TBK1 are essential components of the IRF3 signaling pathway. *Nat. Immunol.* **4**, 491–496 (2003).
35. Fonseca, B.D. *et al.* The ever-evolving role of mTOR in translation. *Semin. Cell Dev. Biol.* **36**, 102–112 (2014).
36. Senesac, J., Gabrilovich, D., Pirruccello, S. & Talmadge, J.E. Dendritic cells transfected with adenoviral vectors as vaccines. *Methods Mol. Biol.* **1139**, 97–118 (2014).

ONLINE METHODS

Mice. Wild-type C57BL/6 and *Goldenticket* STING (*Tmem173*)-deficient mice were obtained from Charles River Laboratories and The Jackson Laboratory, respectively. *Irf3*$^{-/-}$ mice and *Myd88*$^{-/-}$*Trif*$^{-/-}$ mice were bred in a specific pathogen-free environment within the animal facility at McMaster University. All other genotypic mice used for generating bone marrows were as follows: *S6k1*$^{-/-}$, *S6k2*$^{-/-}$, *S6k1*$^{-/-}$*S6k2*$^{-/-}$, *Eif4ebp1*$^{-/-}$*Eif4ebp2*$^{-/-}$ and *Eif4ebp1*$^{-/-}$*Eif4ebp2*$^{-/-}$*Eif4ebp3*$^{-/-}$ mice and control wild-type mice[17,37–39], McGill University; *Irf3*$^{-/-}$, *Myd88*$^{-/-}$, *Mavs*$^{-/-}$ and control wild-type mice[40], Washington University School of Medicine in St. Louis; *Mavs*$^{-/-}$ and control wild-type mice, University of Washington in Seattle; *Tnfr1*$^{-/-}$ *Tbk1*$^{-/-}$ and *Tnfr1*$^{-/-}$ (control for *Tbk1*$^{-/-}$) mice[41], University of Massachusetts Medical School. All animal experiments were approved by the Institutional Animal Research Ethics Board of McMaster University and concurred with the guidelines established by the Canadian Council on Animal Care. No specific exclusion criteria were employed in mouse experiments nor randomization of the allocation of mice to experimental groups was conducted.

BMDC preparation. BMDCs were prepared as previously described[42]. Briefly, bone marrows were flushed from mouse femurs and tibiae and the dissociated bone marrow cells were re-suspended in complete RPMI 1640 in the presence of 55 μM of β-mercaptoethanol (Gibco) and recombinant murine GM-CSF (40 ng/ml; PeproTech). On days 3 and 6, the cultures were provided with new media and fresh GM-CSF. From day 6 to day 8, BMDCs were harvested for various experimental purposes as specified.

Viruses, viral transduction, lipopolysaccharide stimulation and reagents. Recombinant human serotype 5 Ad with deletion of E1–E3 (Ad-BHGdE1E3) harboring no transgene, Ad-OVA expressing chicken ovalbumin peptide SIINFEKL fused to luciferase, and VSV with an M protein mutant (VSV-ΔM51) were described[43]. Ad and Ad-OVA were used at an MOI of 100 whereas VSV was used at an MOI of 25 for the various times as indicated. These MOIs were chosen because they were shown to be effective in transducing DCs for use in DC-based vaccination[43]. HSV-1 (strain KOS) was used at an MOI of 5 for BMDC infection for various time points as specified. Intravaginal infection and titration of infectious HSV-1 progenies were conducted as previously described[44]. Briefly, mice were anaesthetized by injectable anesthetic given intraperitoneally and inoculated intravaginally with 10 μl containing 10^4 PFU of wild-type HSV-1. Vaginal washes were collected 48 h after infection and subjected to standard plaque assays using Vero cells. lipopolysaccharide (*E. coli* O111:B4, Sigma) was used at 100 ng/ml for various time points as specified. Rapamycin was from Calbiochem. Calf intestinal phosphatase (CIP) was from New England BioLabs. Noncanonical 2′,3′ cGAMP (c[G(2′,5′)pA(3′,5′)p]) was purchased from BioLog.

Expression constructs and transfection. HA or Flag-tagged STING was amplified by PCR and cloned into pcDNA3.1 plasmid for expression in mammalian cells. Mammalian expression plasmids encoding HA-tagged wild-type S6K1, kinase-inactive mutant S6K1(K100R) and Myc-tagged wild-type S6K1 and S6K1 truncated versions, as well as expression plasmids for Flag-tagged IRF3, wild-type TBK1 and kinase-inactive mutant TBK1(K38A) were described previously[30,32,45,46]. The expression plasmid for S6K1 with kinase domain deletion, S6K1(ΔKD)-Myc, was made in GenScript. To construct S6K1 C terminus fragment (411-512), the region containing the N terminus, the kinase domain and the linker domain was removed using deletion site directed mutagenesis on pRK5-S6K1-Myc[46]. HEK293T cells were cultured in DMEM supplemented with 10% (v/v) FBS and were transfected using XtremeGENE HP DNA transfection reagent (Roche) according to the manufacturer's instructions for various times as specified.

Lentiviruses. Lentiviral vectors for shRNA silencing of TBK1, cGAS and a scrambled shRNA sequence were obtained from Sigma. The Sigma MISSION shRNA vectors accession numbers were: human TBK1 (TRCN0000314840), mouse cGAS (TRCN0000178625) and the non-targeting scrambled shRNA control (SHC002). Each shRNA vector was co-transfected into HEK293T cells with the lentivirus packaging plasmids PLP1, PLP2, and PLP-VSVG (Invitrogen) using Lipofectamine 2000 (Invitrogen). Viral supernatants were collected 48 and 72 h post-transfection and were filtered through a 0.45 μm nitrocellulose filter before use. For silencing of TBK1 gene expression in HEK293T cells, TBK1 shRNA lentiviral particles were incubated with the cells for 24 h before selection with puromycin and the drug-resistant cells were used for various experiments as indicated. For cGAS silencing, BMDCs collected on day 6 were transduced with cGAS lentiviral particles and were used 48 h later for various experiments as specified. Silencing efficiency was verified by immunoblot analysis.

For lentivirus-mediated transgene expression, wild-type S6K1 and the kinase-inactive version S6K1(K100R) were amplified by PCR and cloned into the lentiviral vector pCW57.1 (Addgene) using NheI and BamHI. Lentiviruses were produced using the PLP1, PLP2 and PLP-VSVG packaging vectors on HEK293T cells and concentrated on sucrose cushion. For the reconstitution experiments, *S6k1*$^{-/-}$*S6k2*$^{-/-}$ BMDCs were transduced on day 3 with lentivirus expressing either wild-type S6K1 or S6K1(K100R). The expressions of the transgenes were induced on day 7 with doxycycline (1 μg/ml). On day 8, the lentivirus-transduced *S6k1*$^{-/-}$*S6k2*$^{-/-}$ BMDCs were used for Ad infection for 24 h.

***In vivo* immunization, T cell preparation and intracellular staining for flow cytometry and VV-OVA challenge.** Following transduction with either Ad-empty or Ad-OVA, the transduced wild-type, *Irf3*$^{-/-}$ or *S6k1*$^{-/-}$*S6k2*$^{-/-}$ BMDCs were injected subcutaneously into the footpads of wild-type recipient mice at 0.5×10^6 cells per footpad. T cell response analysis was conducted as previously described[47]. Briefly, 14 days after immunization, T cells were prepared and incubated with SIINFEKL peptide ($OVA_{257-264}$, Biomer Technologies) at 1 μg/ml for specific T cell restimulation. Incubation was performed for 5 h, in the presence of brefeldin A (GolgiPlug, BD Pharmingen) at 1 μg/ml for the last 4 h. Then, PBMCs were incubated with antibodies against CD16/CD32 (clone 2.4G2, dilution 1:200, BD Biosciences 553142, 1DB-001-0000807496) to block Fc receptors, before T cell surface staining with anti-CD3-APC-Cy7 (clone 145-2C11, dilution 1:100, BD Biosciences 557596, 1DB-001-0000869695), anti-CD8-PE (clone 53-6.7, dilution 1:400, BD Biosciences 553033, 1DB-001-0000868920) and anti-CD4-PerCP-Cy5.5 (clone RM4-5, dilution 1:800, eBioscience 45-0042-82, 1DB-001-0000884856). Cells were permeabilized and fixed with Cytofix/Cytoperm (BD Pharmagen) before intracellular cytokine staining with anti-IFN-γ-APC (clone XMG1.2, dilution 1:100, BD Biosciences 554413, 1DB-001-0000874263) and anti-TNF-α-FITC (clone MP6-XT22, dilution 1:300, BD Biosciences 554418, 1DB-001-0000871919). These antibodies were previously cited[47]. Data were acquired using a FACSCanto flow cytometer with FACSDiva software (BD Pharmingen) and analyzed with FlowJo Mac software (Treestar, Ashland, OR).

On day 26 after immunization with Ad-empty or Ad-OVA-transduced BMDCs, the recipient mice were challenged by i.p. injection of 10^7 PFU of recombinant vaccinia virus encoding an endoplasmic reticulum-targeted SIINFEKL epitope (VV-OVA). Seven days later, VV-OVA titers were determined by plaque assay in the ovaries of the challenged mice[48].

Flow cytometry analysis of BMDCs and lymph node cells. CFSE (5-(and -6)-carboxyfluorescein diacetate succinimidyl ester) was obtained from Sigma. BMDC labeling with CFSE was conducted as previously described[49]. The popliteal lymph nodes were collected 48 h after mock injection or injection of the CFSE-labeled BMDCs into the footpad. Stained BMDCs and lymph node cell suspensions were prepared for cytometry analysis using the flow cytometer and software as stated above. The monoclonal antibody 25-D1.16 was obtained from eBioscience (#17-5743-80) and CD11c antibody was purchased from BD Biosciences (PE-Cy7 CD11c, #558079).

Immunofluorescence microscopy. For immunofluorescence staining, BMDCs were grown on coverslips. After Ad transduction for 24 h, the transduced cells were fixed in cold methanol for 10 min, washed in PBS and blocked in 5% normal goat serum for 45 min. A rabbit anti-mouse IRF3 antibody (#4302, Cell Signaling Technology) was then applied at room temperature for 1 h. After washing in PBS, the cells were incubated with fluorescence-conjugated goat anti-rabbit IgG (Jackson ImmunoResearch Laboratories) for 45 min. Thereafter, the nuclear DNA of the immunolabeled cells were counterstained with DAPI (4′,6-diamidino-2-phenylindole, dihydrochloride, Molecular

Probes) according to the product specification. The fluorescence staining was examined with an LSM 510 META inverted confocal microscope (63× oil objective; Carl Zeiss).

Immunoblot and immunoprecipitation. For immunoblot (IB) analysis, the treated cells were lysed in radioimmunoprecipitation buffer (RIPA) (10 mM phosphate pH 7.4, 137 mM NaCl, 1% NP-40, 0.5% sodium deoxycholate and 0.1% SDS) supplemented with protease inhibitor cocktail (Roche) and phosphatase inhibitor cocktail II and III (Sigma). The preparation of cytoplasmic and nuclear extracts was conducted as previously described[50]. Total or fractionated cellular extracts were resolved on 7.5–12% SDS-PAGE and transferred to nitrocellulose membrane (Santa Cruz). Blots were blocked in Odyssey blocking buffer (Li-cor) unless otherwise specified and detection was performed with respective primary antibodies, and bands were visualized with infrared dye-conjugated secondary antibodies using Odyssey scanner (Li-cor). For immunoprecipitation (IP), the treated cells were lysed in IP buffer (20 mM Tris-HCl pH 7.4, 137 mM NaCl, 1 mM EDTA, 1% NP-40, 10% glycerol and protease/phosphatase inhibitor cocktail from ThermoFisher Scientific, #78441). The cellular extracts were incubated with respective IP antibodies or IP antibodies conjugated to Sepharose beads at 4 °C for 1-3 h or overnight as specified. The immunoprecipitates were washed thoroughly and boiled in SDS sample buffer for western blot analysis.

***In vitro* kinase assay for S6K1-STING-TBK1 complex formation.** To obtain the required recombinant proteins, single transfections of S6K1-HA, STING-Flag and TBK1-Flag were conducted with Lipofectamine 2000 in HEK293T cells for 56 h. The respective recombinant proteins were isolated using HA tagged protein purification kit (MBL, #3320A) and Flag tagged protein purification kit (MBL, #3325A) according to the product specifications. S6K1-HA or STING-Flag or TBK1-Flag was released from respective tag antibody-Sepharose beads with free HA or Flag peptides to retain maximal biological activities. S6K1-HA alone or the reaction mixtures of S6K1-HA and STING-Flag with or without TBK1-Flag were then incubated in 1× kinase buffer (Cell Signaling Technology, #9802) at 30 °C for 1 h in the presence of ATP (Cell Signaling Technology, #9804) at a final concentration of 200 µM. In some experiments, the kinase reactione with STING-Flag and TBK1-Flag were conducted at 30 °C first and S6K1-HA was added at 4 °C later for 1 h. Thereafter, IP buffer (300 µl containing protease/phosphatase inhibitor cocktail from ThermoFisher Scientific, #78441) was added at 4 °C. To avoid the interference with the subsequent IP reactions by free HA or Flag peptides in the reaction mixtures from the competitive elution process, the IP reactions were conducted with rabbit anti-S6K1 antibody (Millipore, #05-781R) for 1 h and the S6K1-antibody complexes were precipitated with anti-rabbit IgG F(ab′)2 fragment Sepharose (Cell Signaling Technology #3400) for 1 h at 4 °C. The immunoprecipitates were analyzed by immunoblot analysis using anti-Flag or anti-S6K1 antibody as indicated.

Antibodies. The primary antibodies used for immunoblot analysis and IP were from the following sources: abcam: IFIT1 (ab11821); Cell Signaling Technology: phospho-TBK1 (#5483), TBK1 (3504), phospho-IRF3 (S396, #4947), IRF3 (#4302), STING (#3337), STING (#13647), p70S6K1 (#9202), phospho-p70S6K1 (Ser371, #9208), phospho-p70S6K1 (Thr389, #9234), phospho-S6 ribosomal protein (S240/244, #5364), S6K2 (#14130), MyD88 (#4283), IPS-1(#4983), ISG15 (#2743), cGAS antibody (#31659), HA-Tag antibody-Sepharose (#3956), HA-Tag antibody (#3724), HA-Tag antibody (#2367), Flag-Tag antibody-Sepharose (#5750), Flag-Tag antibody (#2368), Flag-Tag antibody (#8146), anti-rabbit IgG F(ab′)2 fragment Sepharose (#3400),, Myc-Tag antibody (#2278), GFP-Tag antibody (#2956); Abiocode: cGAS (R-3252-1); Santa Cruz Biotechnology: IRF3 (sc-9082 and sc-15991), TBK1 (sc-9910), histone H1 (sc-10806), p70S6Kβ (S6K2, sc-9381), rabbit anti-goat IgG-HRP (sc-2768), HA-probe (sc-7392), Myc-Tag antibody-Sepharose (sc-40 AC), luciferase antibody (sc-74548); Sigma: β-actin antibody (A5441); Millipore: p70S6K1 (05-781R); Novus Biologicals: TRIF (NB-120-13810); and Zymed Laboratories: IRF3 (ZM3, 51-3200); Rockland Immunochemicals: anti-Flag antibody (#600-401-383).

37. Colina, R. *et al.* Translational control of the innate immune response through IRF-7. *Nature* **452**, 323–328 (2008).
38. Le Bacquer, O. *et al.* Elevated sensitivity to diet-induced obesity and insulin resistance in mice lacking 4E-BP1 and 4E-BP2. *J. Clin. Invest.* **117**, 387–396 (2007).
39. McWhirter, S.M. *et al.* IFN-regulatory factor 3-dependent gene expression is defective in Tbk1-deficient mouse embryonic fibroblasts. *Proc. Natl. Acad. Sci. USA* **101**, 233–238 (2004).
40. Daffis, S., Suthar, M.S., Szretter, K.J., Gale, M. Jr. & Diamond, M.S. Induction of IFN-β and the innate antiviral response in myeloid cells occurs through an IPS-1-dependent signal that does not require IRF-3 and IRF-7. *PLoS Pathog.* **5**, e1000607 (2009).
41. Bonnard, M. *et al.* Deficiency of T2K leads to apoptotic liver degeneration and impaired NF-κB-dependent gene transcription. *EMBO J.* **19**, 4976–4985 (2000).
42. Boudreau, J.E. *et al.* IL-15 and type I interferon are required for activation of tumoricidal NK cells by virus-infected dendritic cells. *Cancer Res.* **71**, 2497–2506 (2011).
43. Boudreau, J.E. *et al.* Recombinant vesicular stomatitis virus transduction of dendritic cells enhances their ability to prime innate and adaptive antitumor immunity. *Mol. Ther.* **17**, 1465–1472 (2009).
44. Konno, H., Konno, K. & Barber, G.N. Cyclic dinucleotides trigger ULK1 (ATG1) phosphorylation of STING to prevent sustained innate immune signaling. *Cell* **155**, 688–698 (2013).
45. Zhao, T. *et al.* The NEMO adaptor bridges the nuclear factor-κB and interferon regulatory factor signaling pathways. *Nat. Immunol.* **8**, 592–600 (2007).
46. Dennis, P.B., Pullen, N., Pearson, R.B., Kozma, S.C. & Thomas, G. Phosphorylation sites in the autoinhibitory domain participate in p70(s6k) activation loop phosphorylation. *J. Biol. Chem.* **273**, 14845–14852 (1998).
47. Pol, J.G. *et al.* Maraba virus as a potent oncolytic vaccine vector. *Mol. Ther.* **22**, 420–429 (2014).
48. Bassett, J.D. *et al.* CD8+ T-cell expansion and maintenance after recombinant adenovirus immunization rely upon cooperation between hematopoietic and nonhematopoietic antigen-presenting cells. *Blood* **117**, 1146–1155 (2011).
49. Parish, C.R., Glidden, M.H., Quahm, B.J.C. & Warren, H.S. Use of the Intracellular Fluorescent Dye CFSE to Monitor Lymphocyte Migration and Proliferation. *Curr. Protoc. Immunol.* **84**, 4.9:4.9.1–4.9.13 (2009).
50. Manel, N. *et al.* A cryptic sensor for HIV-1 activates antiviral innate immunity in dendritic cells. *Nature* **467**, 214–217 (2010).

doi:10.1038/ni.3433